Geocarto International

ISSN: (Print) (Online) Journal homepage: https://www.tandfonline.com/loi/tgei20

Evaluating the impact of land use and land cover change on unprotected wetland ecosystems in the arid-tropical areas of South Africa using the Landsat dataset and support vector machine

Kgabo Humphrey Thamaga, Timothy Dube & Cletah Shoko

To cite this article: Kgabo Humphrey Thamaga, Timothy Dube & Cletah Shoko (2022): Evaluating the impact of land use and land cover change on unprotected wetland ecosystems in the arid-tropical areas of South Africa using the Landsat dataset and support vector machine, Geocarto International, DOI: 10.1080/10106049.2022.2034986

To link to this article: https://doi.org/10.1080/10106049.2022.2034986

GEOCARTO INTERNATIONAL
https://doi.org/10.1080/10106049.2022.2034986

Taylor & Francis
Taylor & Francis Group

Evaluating the impact of land use and land cover change on unprotected wetland ecosystems in the arid-tropical areas of South Africa using the Landsat dataset and support vector machine

Kgabo Humphrey Thamaga[a], Timothy Dube[a] and Cletah Shoko[b]

[a]Institute of Water Studies, Department of Earth Science, University of the Western Cape, Bellville, South Africa; [b]Division of Geography, School of Geography, Archaeology and Environmental Studies, University of Witwatersrand, Johannesburg, South Africa

ABSTRACT

The study explored the impact of Land Use and Land Cover (LULC) change dynamics in relation to the condition and status of an unprotected wetland located in the arid-tropical parts of the Limpopo Province, South Africa. The long-term Landsat archival data series was used to map and quantify the impacts of LULC change on the wetland over a period of 36 years (1983–2019). A multi-source satellite image analysis was performed, using the support vector machine (SVM) algorithm and advanced spatially-explicit geographic information system tools. Landsat data series covering the entire study area was used to assess, map and monitor LULC change that occurred over-time. Post-classification maps for the Maungani wetland area were analysed to provide a quantitative assessment and a detailed overview of the rate of change. The generated wetland detection maps for four temporal phases (i.e., 1983–1992, 1992–2001, 2002–2010) were analysed. This study found that the spatial extent of the wetland area declined severely during the period under study with 728 300 ha. The findings of this work provide critical insights and baseline information about the state of unprotected wetlands in the rural parts. This information is useful for the development of tailor-made wetland management strategies and a possible rehabilitation framework for unprotected wetland ecosystems.

ARTICLE HISTORY
Received 7 June 2021
Accepted 23 January 2022

KEYWORDS
Drivers of wetland conversion; rural development; support vector machine; temporal change; wetland degradation

1. Introduction

Most wetlands are located adjacent to Lakes or fountains and are characterised by hydric soils that experience wet saturation conditions, either during the rainy season, and all year round (Adeli et al. 2020; Tiner et al. 2015). Although wetlands occupy approximately 6% of the earth's surface, they are among the most productive and ecologically diverse ecosystems globally. In their natural condition, wetlands support many environmental and socio-economic services to the neighbouring communities, which are, to some extent,

CONTACT Kgabo Humphrey Thamaga hkgaboreba@gmail.com

largely controlled by the variations in inundation and soil saturation patterns (Dubeau et al. 2017; Thamaga et al. 2021). These ecosystems play a critical role by controlling floods, moderating micro-climates, maintaining and improving the water quality and protecting against erosion (Calhoun et al. 2017; Chandler et al. 2017; Materu et al. 2018). In sub-Saharan Africa, wetlands provide a basis for human livelihoods of many communities living around these ecosystems (Horwitz and Finlayson 2011; Rebelo et al. 2010). For example, communities around the Yala Swamp in Western Kenya were found to depend on it for drinking, cooking and washing, while 86% of the population relied on it for the building materials that are gathered from the wetland, such as clay, sand, wood and papyrus (Schuyt 2005). It was noted that in areas with a strong seasonal and interannual hydro-climatic variability, wetland inundation provides suitable conditions for perennial crop production particularly in arid-tropical environments. Most arid-tropical regions experience erratic rainfall patterns, which lead to crop failure, and hence, there has been a shift towards the utilisation of wetlands, which are characterised by fertile soils and optimal moisture conditions for the sustenance of rural livelihoods.

Despite these benefits, wetlands in the arid-tropical regions remain the most fragile and frequently threatened ecosystems, by both natural and anthropogenic processes. Natural processes, such as global warming, discharge patterns, precipitation changes and extreme weather conditions expedite wetland degradation (Malak and Hilarides 2016; Mohammadimanesh et al. 2018; Singh et al. 2016). In sub-Saharan Africa, for example, the rising water scarcity, as well as prolonged and severe droughts, serve as major threats to wetland ecosystems. Unprotected wetlands are increasingly vulnerable to changes in the population patterns and are frequently affected by the LULC processes. The conversion of wetlands to agricultural land threatens the eco-hydrological functions of wetlands, particularly when large-scale drainage alterations occur (Chen et al. 2020; Mohammadimanesh et al. 2018). According to Symeonakis and Drake (2004), the degradation of upland fields and the increasing change in rainfall due to climate variation, pushes farmers to cultivate crops in wetland areas, where water is readily-available for crop irrigation. The conversion of wetlands, particularly small wetlands, into agricultural land and settlements, is expected to occur on flat terrains or in areas with a gentle slope, as they are largely suitable for crop cultivation and the construction of infrastructure. When land is transformed, small patches of wetlands are likely to disappear in the converted area, depending on the rate of conversion. Siachalou et al. (2014) highlighted that the conversion of land to agricultural fields and settlement spaces for development, limits the geographical scale of wetland areas, while complicating their ecological functions. A study conducted by Van Asselen et al. (2013) revealed that development, economic growth and population density are the main causes of wetland transformation and the most frequently observed factors that perpetuate the degradation process. This is consistent with studies by Lambin and Meyfroidt (2010), Nkonya et al. (2016) and IPBES (2018), who noted that the over-exploitation of natural resources and unregulated infrastructure development placed much pressure on wetland ecosystems, due to the unsustainable utilisation of wetland ecosystems, leading to a great loss of ecological functions. These threats disrupt the ecohydrological stability of wetlands and have major consequences, such as an increase in wetland degradation which contributes to the destruction of wetland ecosystems. The rate of wetland degradation in arid-tropical areas therefore require accurate, continuous and up-to-date information about the extent and status of the condition of wetlands, particularly unprotected wetland systems, to help comprehend the spatio-temporal pattern of the existing land use and land cover activities in the proximity of wetland systems.

Details on the spatio-temporal extent of unprotected wetlands, as well as their status, remain scanty, especially on a localised scale in Sub-Saharan Africa (Lee et al. 2001). As a result, quantifying wetland conversion patterns and land cover classification, over a smaller to a larger spatial scale is critical for understanding their distribution and health status. Due to their remoteness, vastness, and their highly dynamic nature, field-based measurements for the continuous monitoring of wetlands remain impractical, especially in data-scarce environments. These methods are further costly, time-consuming, labour-intensive and they lack spatial representation, given the size of the wetland (Adeli et al. 2020; Gallant 2015). Furthermore, Adam and Mutanga (2009) and Lin et al. (2018) have indicated that sampling errors have proved to be a major drawback when collecting wetland data, commonly due to their inaccessible location. Therefore, given the inaccessibility of in-situ wetland data, there is a pressing need to establish suitable and reliable tools that have the appropriate spatial and temporal scales and monitoring capabilities.

Remote sensing remains the critical alternative tool for addressing the challenging task involved with ground-based methods. It renders an operational, repeatable and integrated mapping framework that screens the spatial degree and condition of wetlands across small to larger landscapes (Lin et al. 2018). Remote sensing satellite imagery enables access to the historical and up-to-date information that is needed to characterize wetland ecosystems; it provides an inventory for monitoring and evaluating the impacts of LULC changes on unprotected wetlands, and it is also a practical and cost-effective means of doing so (Robertson et al. 2015). Satellite mapping helps to identify baseline information on ecosystem health of wetlands, to diagnose the threats and pressures to wetlands, to monitor any changes in their magnitude and state to inform enhanced decision-making and management strategies.

Thus far, several studies have used various satellite datasets for wetland characterization, as well as for monitoring, mapping and assessing the associated LULC changes over time, at varying spatial and temporal resolutions (Lin et al. 2018; Munishi and Jewitt 2019). Satellite imagery, such as Landsat, ASTER, SPOT, AVHRR and MODIS, provide long-term spatial data archives for ecological assessment, monitoring and management purposes (Muavhi and Mavhungu 2020). These images have been used in various studies, for example, on LULC change, wetland monitoring and extent mapping, biomass estimation and mapping, soil moisture applications, inundation mapping and water level monitoring (Basu et al. 2021; Chatziantoniou et al. 2017; Connolly 2018; Ligate et al. 2018; Mudereri et al., 2019; Munishi and Jewitt 2019; Slagter et al. 2020; Yirsaw et al. 2017), amongst others. In the above-mentioned studies, several techniques such as maximum likelihood, support vector machine, artificial neural network, CART, random forest, object-based image analysis and decision tree were applied to assess wetland changes. On the other hand, Mansaray et al. (2019) compared support vector machine and random forest to map paddy rice in China. The results showed that SVM outperformed RF by achieving overall classification accuracies of 90.80% and 89.20%. Goodin et al. (2015) used Landsat 8 and SVM classifier to assess six land cover classes. The results obtained from their study achieved a relative overall accuracy of 88%. In addition, Hettiarachchi et al. (2015) used Landsat images to map wetland degradation, and the findings revealed that urbanization, industrialization and the expansion of agriculture were the major threats influencing wetland degradation. In contrast, Bassi et al. (2014) found that the loss of the spatial extent of wetlands in India was due to the rapid population growth in the remote areas. The performance of SVM in detecting and classifying wetlands achieved higher accuracies and this provide an effective and promising method for identification and classification of small wetlands.

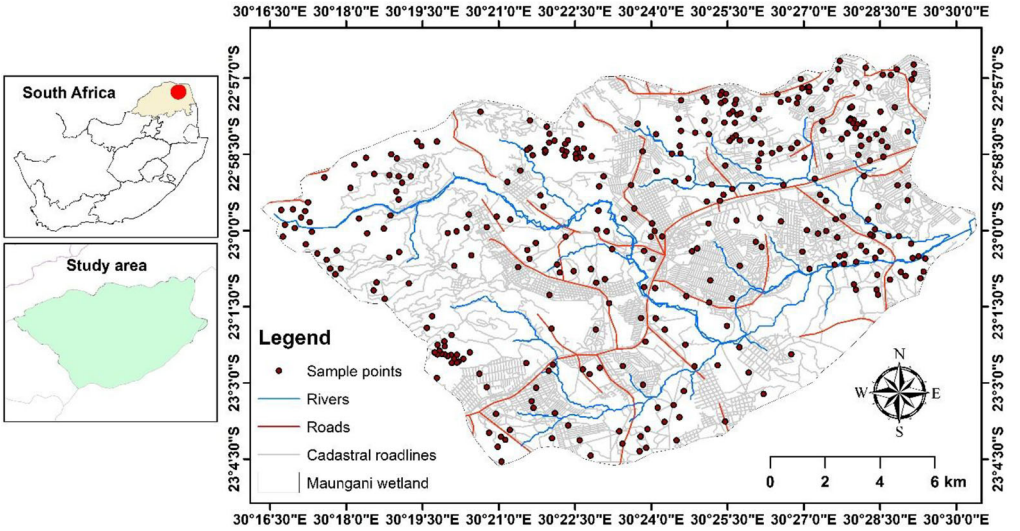

Figure 1. Map of the Maungani wetland in the Limpopo province of South Africa.

In this study, we therefore hypothesized that, determining the past and present status of unprotected wetlands could help and guide environmental managers in their efforts to conserve wetland areas in a sustainable manner. Previous studies related to wetland monitoring, mapping and assessment have only focused on large wetlands that are designated under the Ramsar Convention, and they neglect unprotected wetlands (non-Ramsar), which are also of global importance. Thus, this study aimed at investigating the impacts of LULC change dynamics on the condition and status of the unprotected Maungani wetland, using the Landsat data series, as well as geospatial techniques, such as statistical analysis and Support Vector Machines (SVM), and to measure the LULC changes that affected the Maungani wetland during the 1983 to 2019 period (36 years). We therefore assume that the findings of this study will enhance the capacity and knowledge of environmental managers, policymakers, and local governments, in order to minimize the human footprint on unprotected wetlands in semi-arid tropical areas, particularly in sub-Saharan Africa.

2. Materials and methods

2.1. Study area description

The research was carried-out in Maungani wetland, which is found in the Luvumbu quaternary catchment, Limpopo Province in South Africa. The wetland area is situated between 30°26'30'' E, 22°59'05'' S and 30°25'45'' E, 22°58'45'' S (Figure 1) and occupies an aerial extent of approximately 2 490 700 ha. The Maungani wetland lies adjacent to the Dzindzi River, a tributary of Levuvhu River (Adekola, 2007). Rainfall and temperature are influenced by the Soutpansberg Mountain range. Temperature of the region extends among 18 °C and 37° C, with the mean annual precipitation ranging from 7 mm to 642 mm each year. Vegetation distribution is strongly influenced by altitudinal gradient, with mixed vegetation types occurring on the highest elevations with Acacia-Themeda bush on the plains. Several seasonal streams exist, and these quickly dry as the dry season sets. The wetland is characterised by stamp lands, as well as marshy vegetation. Further, it is dominated by *Thelypteris interrupta, Phragmites australis and Eichinochloa pyramidalis*

Table 1. Description of LULC types identified and used in the study.

LULC class	Description of LULC classes
Agriculture	Agricultural or cultivated lands and farmlands.
Built-up	Built-up comprises all developed land, including residential, commercial, and socio-economic infrastructure.
Bare land	This is the area without or with little vegetation cover.
Forest	Land covered with relatively tall tree with at least 20% canopy mainly dominated by shrub lands, forest nursery.
Other vegetation	Mixed grassland, vegetation lands, vegetation on customary land. This class also consist of unmanaged land areas that are not characterised in any of the above classes.
Water	River, streams, and waterbodies.
Wetland	Area is covered with by water and hydrophytic vegetation in either rivers, streams, lakes, or catchments.

plant species, amongst others. The main economic activities in the area are agriculture, livestock rearing and small-scale farming activities. Maungani wetland is home to approximately 618 462 people living in the surrounding communities (STATSSA 2011). The major land cover types in the selected study site include wetland vegetation, water, other vegetation, built-up, agricultural land and bare land.

2.2. Field data collection

The data used in this study were collected from the 03rd–10th of October 2019 (Figure 1). This period was selected because of its suitability to detect, to discriminate, and thereafter to distinguish, the wetland from other vegetation species in the area. During the field data collection, the Trimble hand-held Global Position Systems (GPS) at submeter accuracy were used to record LULC feature coordinates within the Maungani wetland. A total of 350 sample points (50 per land cover class) were randomly collected, and they are detailed in Table 1. In addition, these data were used to validate the LULC classification and evaluate the precision of classified images. The sample locations of LULC were created, using Hwath's analysis in a GIS environment and they were then imported into the Trimble GPS, in order to navigate us to the specified spots.

2.3. Satellite image acquisition and pre-processing

Field data that coincide with remote sensing satellite data (Landsat 5 TM and 8 OLI: see Table 2) were attained and used to investigate the LULC, as well as change dynamics of the Maungani wetland for 36-years. Landsat satellite images were selected because they have sufficient long archival data, they are freely accessible and because of their reported performance in other land cover classifications and wetland analysis studies (Fashae et al. 2020; Jin et al. 2017). For this study, five scenes of cloudless Landsat 5 TM and one Landsat 8 OLI satellite imagery time-series data, dating from 1983 to 2019, with 9-year intervals, covered the study area, and they were acquired from the United States Geological Survey (USGS) data portal (http://glovis.usgs.gov).

Preceding to the classification process, Landsat images were imported into the ENVI software (Harris Geospatial Solutions, Herndon, VA, USA, version 5.3). The Fast Line-of-sight Atmospheric Analysis of Spectral Hypercube (FLAASH) radiative transfer model for

Table 2. Details of acquired satellite data.

Satellite	Sensor ID	Date	Image acquisition	Source
Landsat 4	TM	1983	LT04_L1TP_169076_19830903_20170220_01	USGS website
Landsat 5	TM	1992	LT05_L1TP_169076_19921030_20170120_01	USGS website
	TM	2001	LT05_L1TP_169076_20010917_20161210_01	USGS website
	TM	2010	LT05_L1TP_169076_20101106_20161015_01	USGS website
Landsat 8	OLI	2019	LC08_L1TP_169076_201911005_20200110_01	USGS website

atmospheric corrections was applied to images during the study period to remove impurities (Mushore et al. 2016). Images were orthorectified and geometrically corrected by using ground control points (GCPs). Selected bands from Landsat images (Tables 3 and 4) were also used. Bands: 1 (coastal aerosol), 6 and 7 (thermal band), 9 (water vapour), 8 (panchromatic), 9 (SWIR – cirrus), 10 (LWIR-1) and 11 (LWIR-2) were excluded from the analysis, due to their spatial resolution (60 and 120 m) and their relevance relating to the detection of atmospheric features (Drusch et al. 2012; Hagolle et al. 2015). The spectral bands have been considered to be inapplicable in vegetation monitoring (Immitzer et al. 2016). The Blue, Green, Red, NIR and SWIR 1 and 2 bands were used in this study.

3.4. Image classification

The Support Vector Machine (SVM) classifier embedded in ENVI 5.3 was used to assess the impacts of LULC changes affecting the Maungani wetland for the years 1983, 1992, 2001, 2010 and 2019. The SVM is a supervised, non-parametric statistical machine learning technique that has been shown to be suitable for image classification challenges with larger dimensionality (Licciardi et al. 2009). Comparative studies assessed the performance of supervised classifiers and found that SVM classifier produced higher accuracy results than other supervised classifiers such as Maximum Likelihood, Mahalanobis Distance, Minimum Distance, Spectral Angle mapper, Random Forest (Jia et al. 2014; Muavhi 2020). The SVM Classifier appear to be advantageous in the presence of heterogeneous classes for which only few training data are used than other machine learning classifiers which require additional training dataset as the input dimensionality increases (Muavhi 2020; Yu et al. 2013). It locates the optimal hyper-plane between two classes to separate them in a new high-dimensional feature space by taking into account only the training samples that lie on the margin of the class distributions known as support vectors. The SVM, is a method produced to solve pattern recognition and nonlinear function estimating problem (Sahu et al. 2015). SVM was implemented using the Radial Basis Function (RBF) kernel characterised by default gamma of 0.33, penalty parameter of 100.00, pyramid level was set at 0 and classification probability threshold was also 0. Although its performance was tested on large scale mapping, using SVM in this study will provide a clear view on the rate of small wetland status.

2.5. Classification accuracy assessment

The derived LULC change maps for the years 1983, 1992, 2001, 2010 and 2019 were assessed for classification accuracy assessment. The field data samples were divided into 70% training (245 points) and 30% testing (105 points). The principle behind separating data into 70%/30% is because they represented a large training data set, while the remaining data was preserved to compute accuracy statistics (Adelabu et al. 2014; Adjorlolo et al. 2013). An error matrix was used to assess the accuracy of the classification process (the overall, user and producer accuracy) relative to the reference data. Further, the error

Table 3. 2015–2019 Landsat 8 OLI band specification used for 2019.

Band name	Centre of electromagnetic region (μ)	GSD(m)
1. Coastal/Aerosol	0.433–0.453	30
2. Blue	**0.452–0.512**	**30**
3. Green	**0.533–0.590**	**30**
4. Red	**0.636–0.673**	**30**
5. NIR	**0.851–1.879**	**30**
6. SWIR – 1	**1.566–1.651**	**30**
7. SWIR – 2	**2.107–2.294**	**30**
8. Panchromatic	0.500–0.680	15
9. Cirrus	1.360–1.390	30
10. LWIR-1	10.6–11.2	100
11. LWIR-2	11.5–12.5	100

*NIR –Near Infra-red, SWIR – Shorter Wave Infrared, LWIR – Lower Wave Infrared. Six bands highlighted in bold were used in the study for analysis.

Table 4. Landsat 5 TM band specification used for the year 1983 and 2010.

Band name	Centre of electromagnetic region (μ)	GSD (m)
1. Blue	**0.45–0.52**	**30**
2. Green	**0.52–0.60**	**30**
3. Red	**0.63–0.69**	**30**
4. NIR	**0.76–0.90**	**30**
5. SWIR – 1	**1.55–1.75**	**30**
6. SWIR – 2	**2.03–2.35**	**30**
7. Thermal	10.40–12.50	120

*NIR – Near Infrared, SWIR – Shorter Wave Infrared. The bolded bands were used in the study and band that is not written in bold is not used for analysis.

matrix provided a comprehensive evaluation of the agreement, omission and commission amongst the classification results and training data, with evidence on how the classification errors occurred (Pontius and Millones 2011).

2.6. Change detection analysis and post classification

Existing LULC classes occupying Maungani wetland were evaluated for the study period and expressed it as the amount of the entire study area. This empowered the assessment and estimation of the LULC changes, within the timeframe between 1983–1992, 1992–2001, 2001–2010, 2010–2019 and 1983–2019. The post classification comparison was used as the change detection technique. This approach is a comparative analysis of satellite images belonging to different times classified as independently from each other. Advantage of this method is that it gives information about the magnitude and direction of change. Although both images come from the same sensor, spectral differences are expected to occur in the same LULC classes due to changes in atmospheric conditions, sun angle, etc. even if the time interval is very small in multi-time data (Munyati 2000). Based on the post classification comparison technique, the change is identified based on pixel-by-pixel basis by overlapping LULC maps belong to different dates obtained by the classification technique. At the end of the process, the number of areas which have undergone change and which class has changed can be identified. Overall change detection maps between 1983 and 2019 were produced to show the LULC conversion. This type of analysis is very much useful in identifying the various changes in the LULC classes, such as an increase in built-up and high rate of decrease in wetland extent. Figure 2 shows a summarised methodological flowchart.

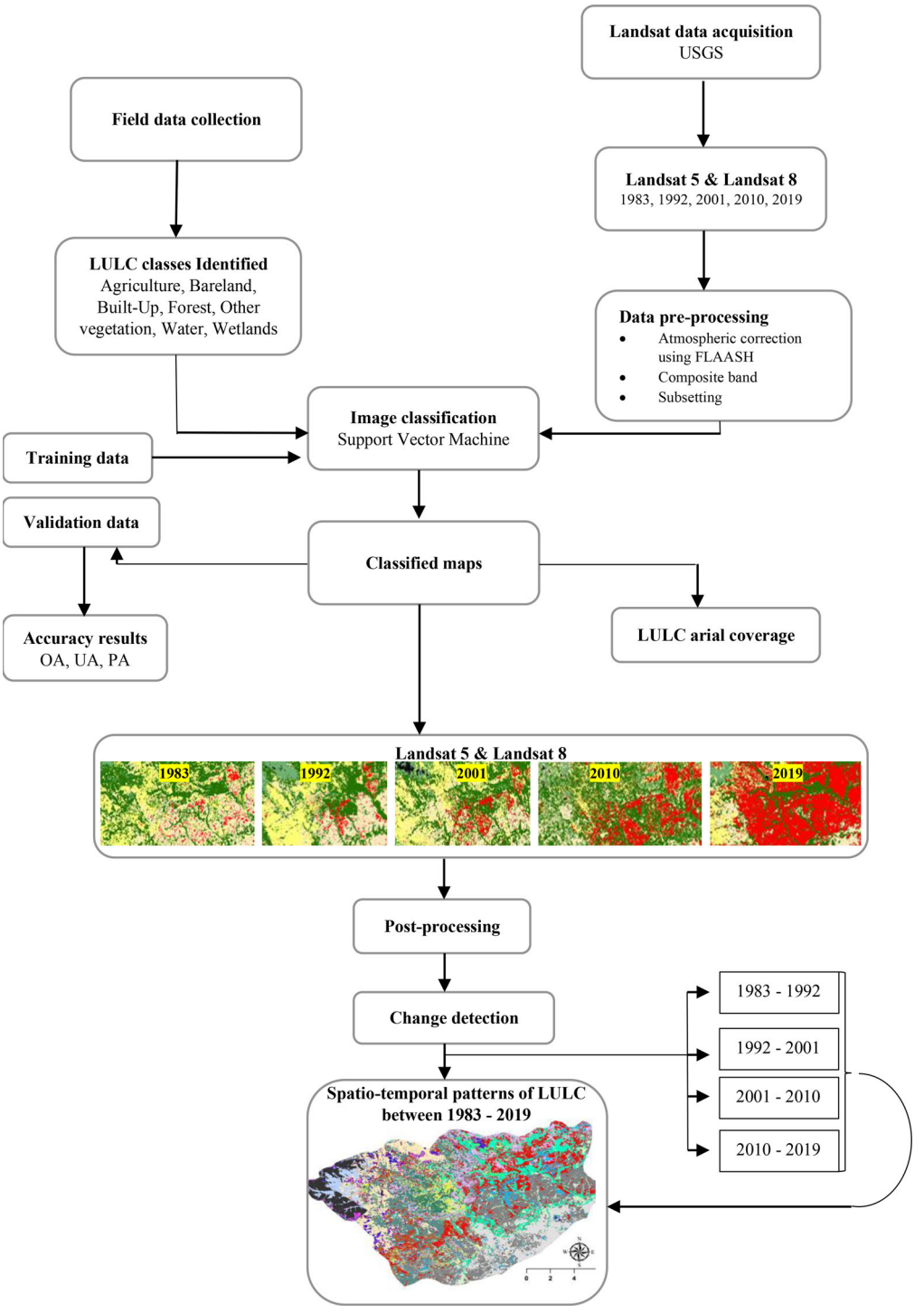

Figure 2. Flow chart showing the methodology.

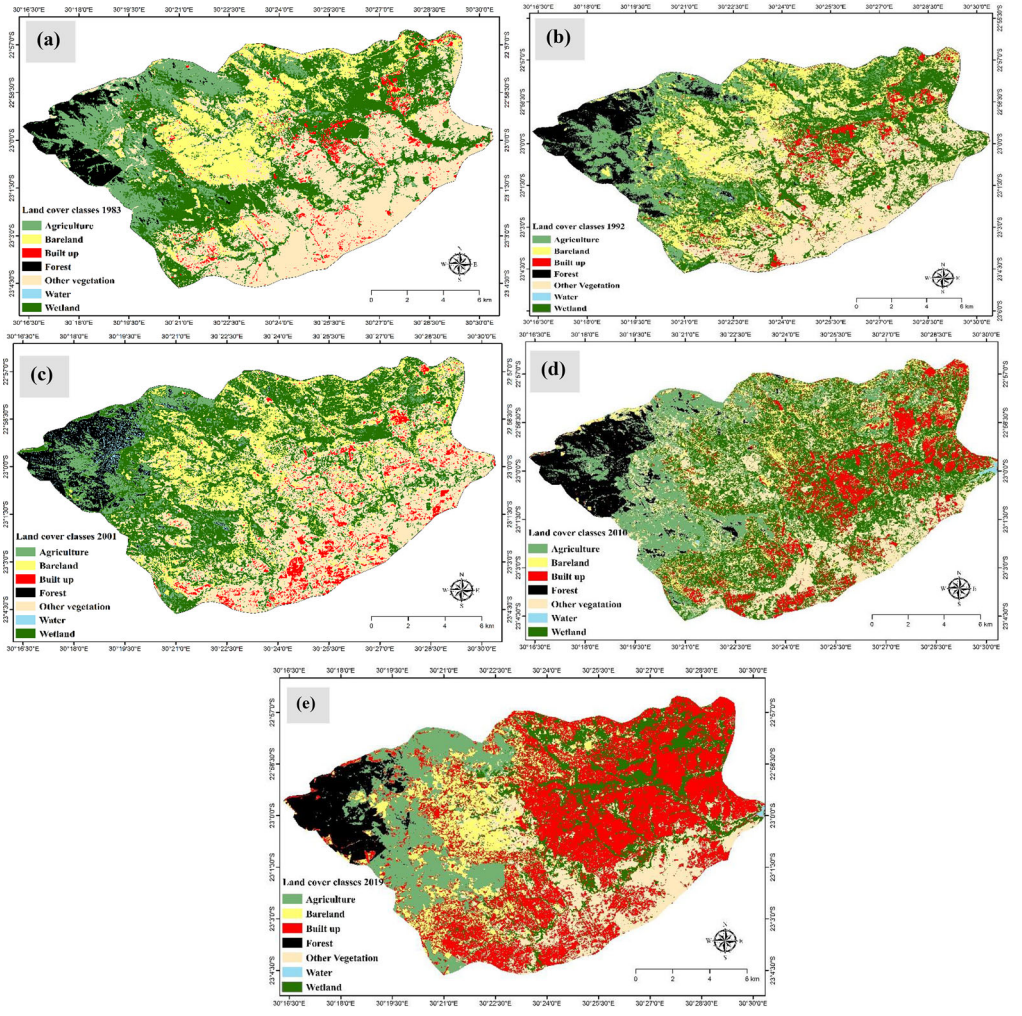

Figure 3. Spatial distributional pattern of identified LULC change maps for: (a) 1983, (b) 1992, (c) 2001, (d) 2010 and (e) 2019.

3. Results

3.1. Satellite derived wetland LULC change (1983–2019)

Derived maps were produced, using SVM, in order to understand the rate of conversion for the periods between 1983 and 2019 (see Figure 3). It was observed that in 1983 the wetland, other vegetation, bare land and agriculture dominated the entire study area. Wetland areas were found in all directions, other vegetation occupied the larger part in the south, and agriculture occupied the western parts of the wetland. In 1992, a considerable portion of agriculture had been converted to forest. Although the wetland covered a larger area in 2001, part of its areal extent was replaced mainly by vegetation or bush encroachment. During 2010 and 2019, there was a sharp increase in the built-up area, which replaced a large portion of the wetland area. In 2010, the area under agriculture increased, when compared to the year 2002, particularly on the western side of the study area. Overall, the maps showed a decline in wetland coverage, which was replaced by built-up areas.

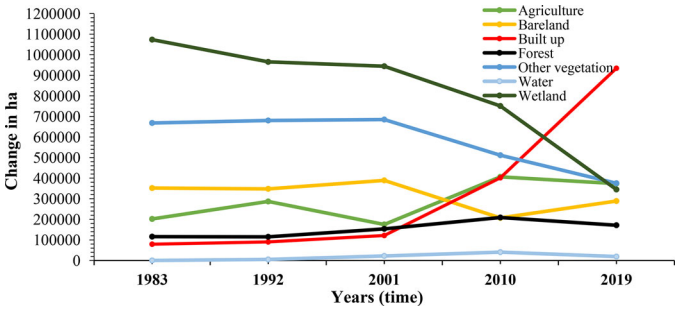

Figure 4. Time series variation of LULC change and wetland dynamics from 1983 to 2019.

3.2. Spatio-temporal change analysis of wetland area overtime

The spatio-temporal change analysis of the wetland area has been presented in Figure 4 and Table 5. During the study period, five (5) thematic maps were derived by using the SVM classifier to assess the change dynamics of the Maungani wetland area for the years 1983, 1992, 2001, 2010 and 2019. This wetland experienced significant change due to anthropogenic activities. In the year 1983, the wetland was the dominant land feature type, covering 43.10% (10 734 900 ha) of the total area, followed by other vegetation that covered 668 400 ha (26.84%). It was also observed that in the western part of the study site, agricultural land occupied an area of about 201 900 ha (8.11%), and in the eastern part, the concentration of built-up areas was 79 100 ha (3.17%). It can be observed from the map that the wetland area decreased by 108 200 ha, to 965 300 ha (38.76%), in 1992, when compared with areal coverage in 1983. Overall, there was an increase in areas with vegetation, in bare land and built-up areas, which covered an area of 680 400 ha (27.32%), 286 800 ha (11.52%) and 90 100 ha (3.62%), respectively. On average, the wetland shrunk greatly, with much of the area being replaced by bushy vegetation (27.32%) in the south towards the eastern part of the study site and bare land (13.97%). It was observed that more than 50% of the wetland area was lost to other land cover classes from 2001, with 944 100 ha (37.90%) of the wetland remaining. Other vegetation covered 685 100 ha, mainly in the east and south of the study site (27.51%), with bare land covering 389 300 ha (15.63%) and a consistent increase in built-up areas, which occupied approximately 121 400 ha (8.87%) of the wetland. In the year 2010, the wetland area remained at 750 900 ha (30.15%), with an increase in the vegetation and built-up areas occupying major parts of the wetland, with an aerial extent of 511 700 ha (20.54%) and 402 000 ha (16.14%), respectively. In addition, during the year 2019, the results revealed that the wetland was impacted by other LULC changes. Only 345 100 ha (13.85%) of the wetland remained unaffected. When compared to the year 1983, the Maungani wetland lost approximately 728 300 ha in 2019. This observation was further confirmed by the results in Figure 4, which show the trends of the wetland change and other LULC changes that occurred within the study area. The overall classification during the study period (1983–2019) showed that the wetland area lost 728 300 ha of its spatial extent to vegetation covered areas with 375 400 ha (15.07%), and built-up areas with 934 300 ha (37.51%).

3.3. Accuracy assessment derived from thematic maps

Based on ground-truth data and Google Earth imagery, the derived satellite images of the wetland area were validated. Between 1983 and 2019, the SVM classifier achieved higher

Table 5. Summary of LULC areal coverage between 1983 and 2019 (area in ha).

	Total change in area									
	1983		1992		2001		2010		2019	
LULC types	Area	%	Area	%	Area	%	Area	%	Area	%
Agriculture	201 900	8.11	286 800	11.51	175 100	7.03	406 400	16.32	373 700	15
Bareland	352 100	14.13	348 100	13.98	389 300	15.63	207 000	8.31	289 000	11.60
Built up	79 100	3.17	90 100	3.62	121 400	8.87	402 000	16.14	934 300	37.51
Forest	115 800	4.65	115 000	4.62	153 700	6.17	208 800	8.38	171 400	6.89
Other vegetation	668 400	26.84	680 400	27.32	685 100	27.51	511 700	20.54	375 400	15.07
Water	100	0.0004	5 000	0.20	22 100	0.89	40 400	0.16	18 900	0.08
Wetland	1 073 500	43.10	965 300	38.75	944 100	37.90	750 900	30.15	345 100	13.85

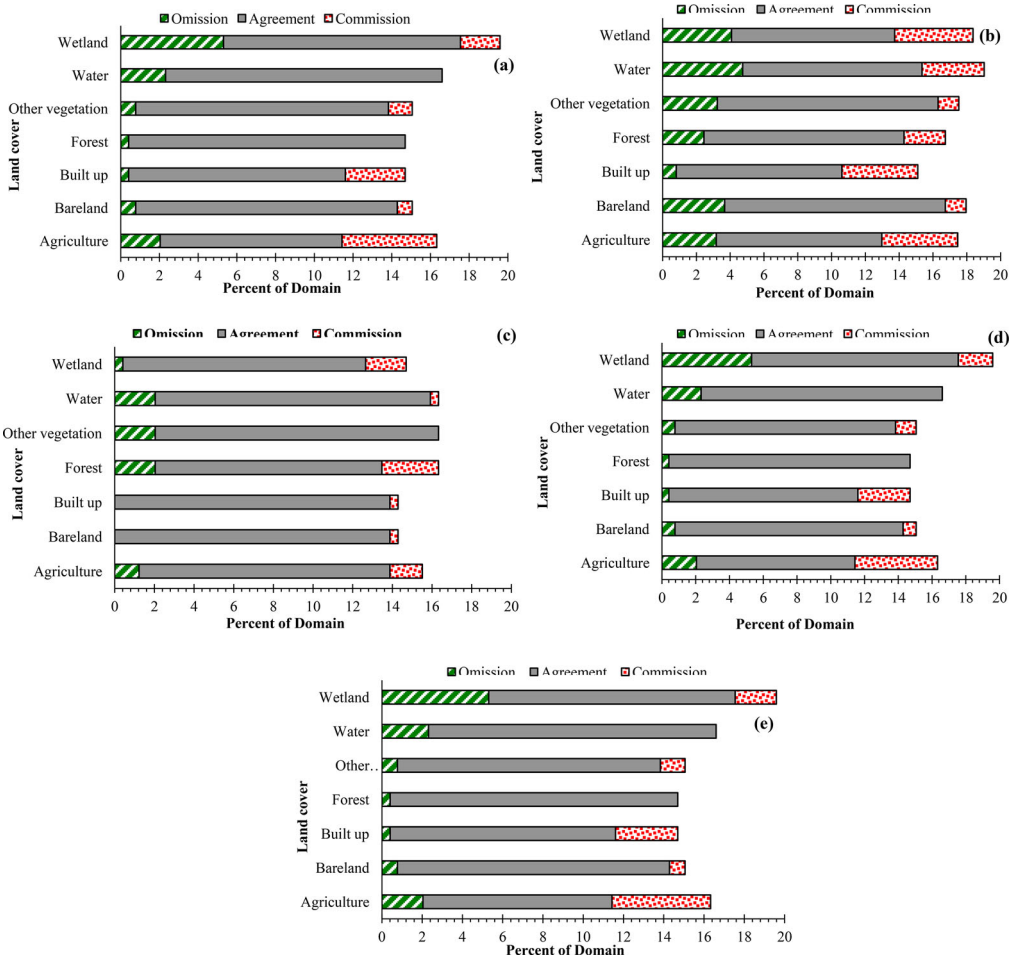

Figure 5. Commission, omission error depicted in (a) 1983, (b) 1992, (c) 2001, (d) 2010 and (e) 2019.

overall classification accuracies, ranging from 77.55% to 92.24% (see Table 6). During the years 1983, 1992, 2001, 2010 and 2019, the overall classification accuracies achieved were 87.76%, 77.55%, 92.24%, 91.43% and 83.67%, respectively, which indicate that there was agreement between the reality on the ground and the satellite-derived images. However,

Table 6: Derived LULC classification accuracies: Overall accuracy (OA), Producer accuracy (PA) and User accuracy (UA) between the year (a) 1983, (b) 1992, (c) 2001, (d) 2010 and (e) 2019.

1983 [a]	Agriculture	Bareland	Forest	Other vegetation	Water	Wetland	built up	Total	UA (%)
Agriculture	23	0	1	0	0	11	0	35	**65.71**
Bareland	0	35	0	0	0	0	0	35	**100**
Forest	0	0	31	0	4	0	0	35	**88.57**
Other vegetation	0	0	0	32	0	2	1	35	**91.43**
Water	0	0	0	0	35	0	0	35	**100**
Wetland	5	0	0	0	0	30	0	35	**85.71**
built up	0	2	0	2	2	0	29	35	**82.86**
Total	28	37	32	34	41	43	30	245	**87.76**
PA (%)	**82.14**	**94.59**	**96.88**	**94.12**	**85.37**	**69.77**	**96.67**		

1992 [b]	Agriculture	Bareland	Built up	Forest	Other vegetation	Water	Wetland	Total	UA (%)
Agriculture	24	0	0	2	1	3	5	35	**68.57**
Bareland	0	32	0	0	3	0	0	35	**91.43**
Built up	0	8	24	0	3	0	0	35	**68.57**
Forest	4	0	0	29	0	2	0	35	**82.86**
Other vegetation	0	0	2	0	32	0	1	35	**91.43**
Water	0	1	0	4	0	26	4	35	**74.29**
Wetland	4	0	0	0	1	7	23	35	**65.71**
Total	32	41	26	35	40	38	33	245	**77.55**
PA (%)	**75**	**78.05**	**92.31**	**82.86**	**80**	**68.42**	**69.79**		

2001 [c]	Agriculture	Bareland	Built up	Forest	Other vegetation	Water	Wetland	Total	UA (%)
Agriculture	31	0	0	4	0	0	0	35	**88.57**
Bareland	0	34	0	0	0	0	1	35	**97.14**
Built up	0	0	34	0	1	0	0	35	**97.14**
Forest	2	0	0	28	0	5	0	35	**80**
Other vegetation	0	0	0	0	35	0	0	35	**100**
Water	0	0	0	1	0	34	0	35	**97.14**
Wetland	1	0	0	0	4	0	30	35	**85.71**
Total	34	34	34	33	40	39	31	245	**92.24**
PA (%)	**91.18**	**100**	**100**	**84.85**	**87.50**	**87.18**	**96.77**		

2010 [d]	Agriculture	Bareland	Built up	Forest	Water	Wetland	Other vegetation	Total	UA (%)
Agriculture	34	0	0	0	0	1	0	35	**97.14**
Bareland	0	31	0	1	1	0	2	35	**88.57**
Built up	0	3	32	0	0	0	0	35	**91.43**
Forest	0	0	0	35	0	0	0	35	**100**
Water	0	0	0	1	34	0	0	35	**97.14**
Wetland	1	1	0	0	0	30	3	35	**85.71**
Other vegetation	0	0	0	0	0	7	28	35	**80**
Total	35	35	32	37	35	38	33	245	**91.43**
PA (%)	**97.14**	**88.57**	**100**	**94.59**	**97.14**	**78.95**	**84.85**		

2019 [e]	Agriculture	Bareland	Built up	Forest	Other Vegetation	Water	Wetland	Total	UA (%)
Agriculture	15	0	0	0	0	20	0	35	**42.86**
Bareland	0	32	0	0	3	0	0	35	**91.43**
Built up	0	2	30	1	1	1	0	35	**85.71**
Forest	0	0	0	32	0	3	0	35	**91.43**
Other Vegetation	0	0	0	0	35	0	0	35	**100**
Water	9	0	0	0	0	26	0	35	**74.29**
Wetland	0	0	0	0	0	0	35	35	**100**
Total	24	34	30	33	39	50	35	245	**83.67**
PA (%)	**62.50**	**94.12**	**100**	**96.97**	**89.74**	**52**	**100**		

in this study, the accuracies of the producers and users generating LULC maps were satisfactory and ranged from 42.86% to 100%, respectively. The commission, agreement, and omission errors (see Figure 5) were found to be the lowest for the year 2001 and ranged between 0% and 3%.

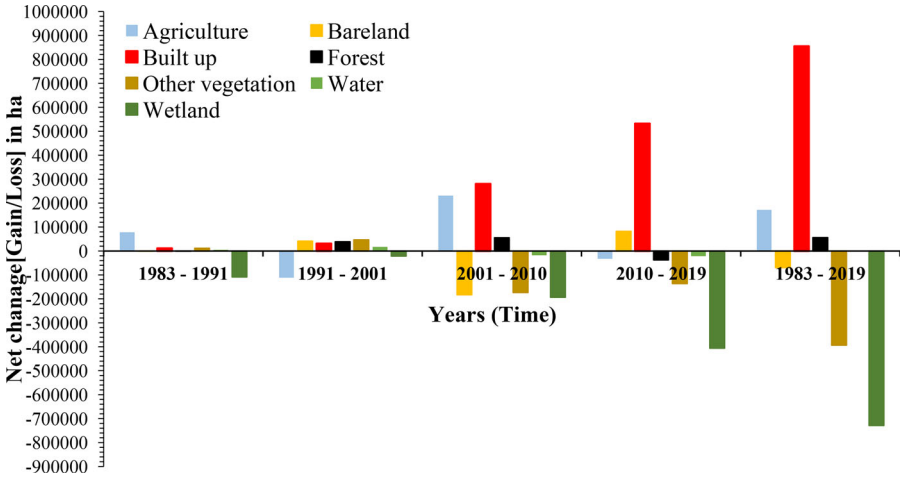

Figure 6. Total area and amount of LULC change (Net change: Gains/losses) on wetland area between 1983 and 2019.

Table 7. LULC change transition between land cover classes 1983 to 2019.

Initial state (1983)/ Final state (2019)	Transition of change between LULC classes						
	Agriculture	Barelands	Built up	Forest	Other vegetation	Water	Wetland
Agriculture	171 800	21 700	296 700	257 900	−294 700	373 700	−699 700
Bareland	87 100	−63 100	209 900	173 200	−379 500	288 900	−784 500
Built up	732 500	582 300	855 300	818 500	265 900	934300	−139 100
Forest	−30 500	−180 700	92 300	55 600	−497 100	171400	−902 000
Other vegetation	173 500	23 300	296 300	259 600	−293 000	375400	−698 000
Water	−2 000	−350 200	−77 200	−113 900	−666 500	11900	−1 071 500
Wetland	143 200	−69 800	266 000	229 300	−323 300	345100	−728 300

3.4. Land use land cover change detection

The spatial information in Figure 6 and Table 7 for the period under study revealed that both gains and losses occurred within the boundary of Maungani wetland boundary. The net-changes, as a result of gains or losses for each LULC type between the years 1983–1992, 1992–2001, 2001–2010 and 2010–2019, are depicted in Figure 6. It was realised that much of the wetland was lost (108 200 ha) between 1983 and 1991, while the agriculture and built-up areas increased by 78 000 ha and 11 100 ha, respectively. Between 1991 and 2001, the agriculture and wetland areas lost 118 200 ha and 71 900 ha, respectively, while the built-up areas (31 300 ha) and bare lands (41 200 ha) gained in their spatial extent. Between 2001 and 2010, the wetland (193 200 ha), bare lands (173 400 ha) and other vegetation (182 300 ha) lost the most spatial extent, whereas between 2001 and 2010, the built-up areas (280 600 ha) and agriculture (231 300 ha) gained a larger proportion. Furthermore, the wetland (405 800 ha) and other vegetation (136 300 ha) suffered the greatest declines between 2010 and 2019. The built-up and agricultural areas covered an aerial extent of 532 400 ha and 82 000 ha, respectively. The wetland lost an aerial extent of about 728 400 ha between 1983 and 2019. The built-up area was found to be the most dominant feature class, occupying 855 300 ha of the total area. In the same period, other vegetation (393 000 ha) lost its spatial coverage over the same time-frame, while agriculture gained coverage by 171 800 ha and 855 300 ha, respectively.

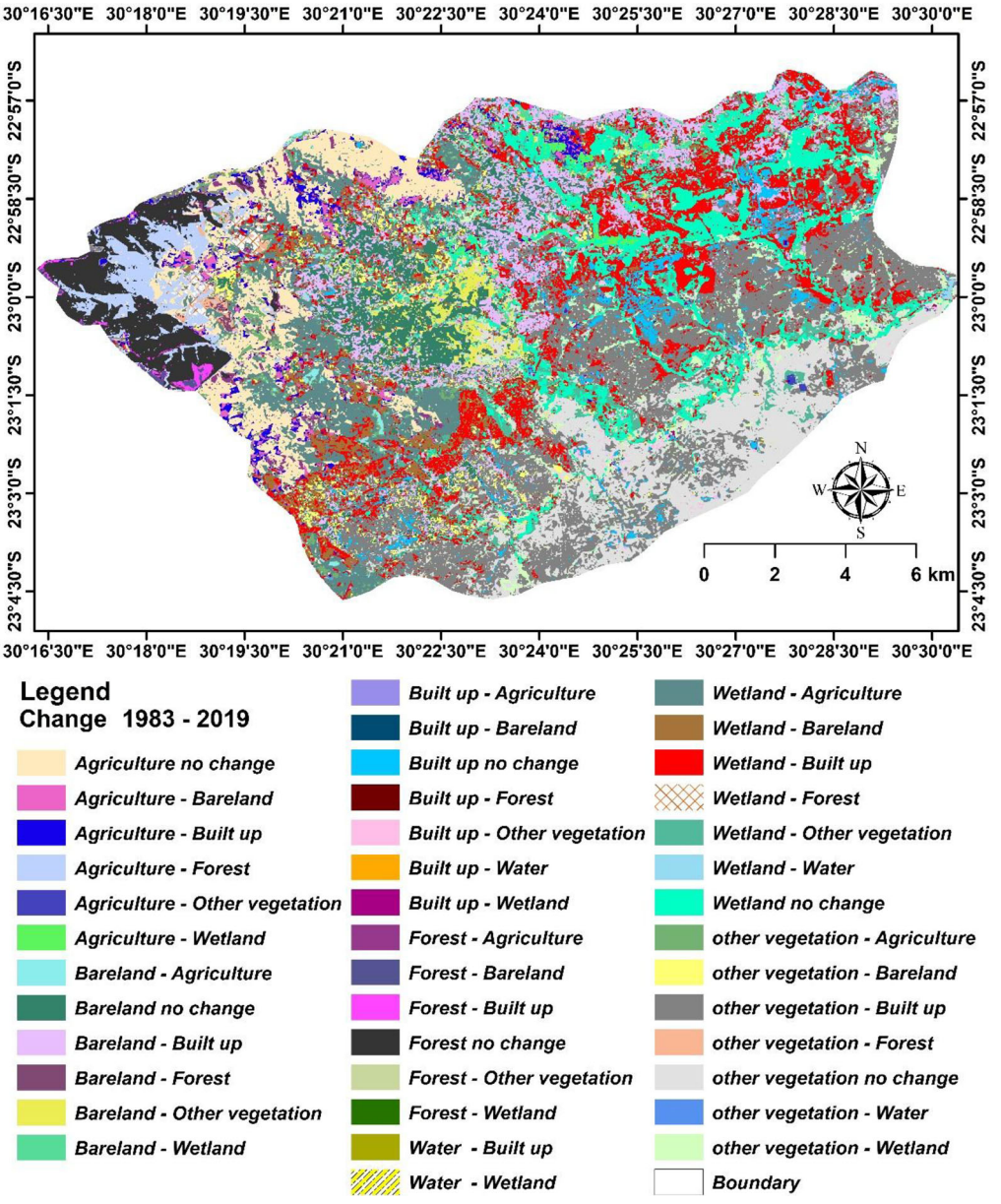

Figure 7. Overall land use land cover conversion during monitoring period (1983 to 2019).

Table 7 demonstrates the percentage loss of wetlands to other LULC types between 1983 and 2019. The spatial extent of wetlands has experienced a massive modification, compared to other LULC types, during the period of study. Over the period of 36 years, 728 300 ha of the wetland area was lost. The majority of the wetland was lost to 784 500 ha of built-up areas and 22.97% of agricultural land. The spatial extent of the Maungani wetland has declined over the years, compared to other LULC types. In Figure 7, it can be observed that there has been a major transformation in the wetland between 1983 and 2019, due to the rapid population growth and anthropogenic activities. In Figure 8, it can be observed that the wetland (2 550.19 ha), other vegetation (4 190.47 ha)

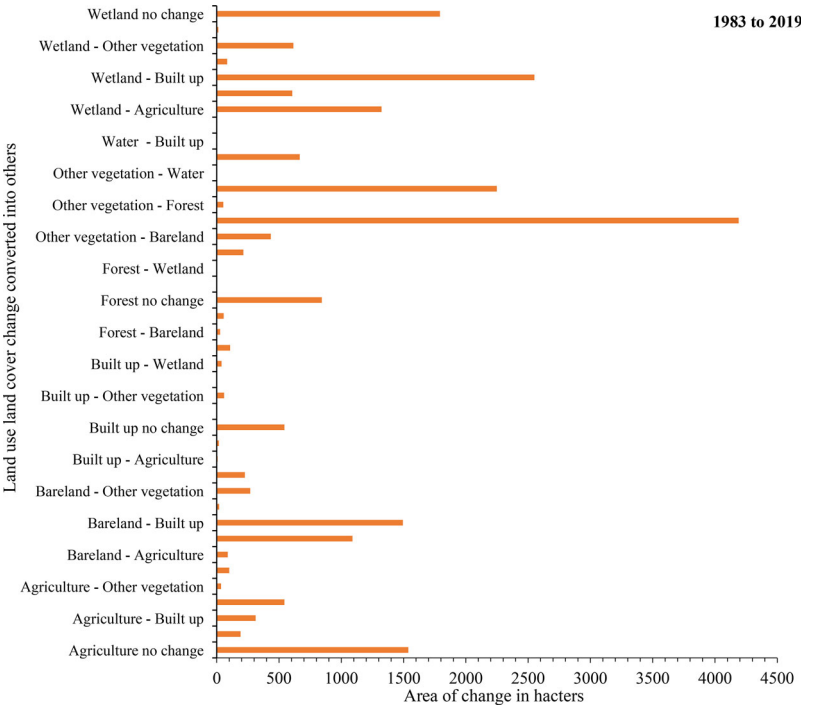

Figure 8. Area of Maungani wetland ecosystem converted into other LULC between 1983 and 2019.

and bare land (1 949.67 ha) were largely converted to built-up areas. The LULC cover transition replaced the wetland area, particularly in the low-lying areas. Pockets of wetland were also converted into other LULC classes.

4. Discussion

The present study investigated the impacts of LULC change dynamics on the unprotected Maungani wetland, which is in the semi-arid tropical regions of the Limpopo Province, South Africa. The freely available Landsat satellite data and Support Vector Machine enabled the study of the wetlands and LULC changes between 1983 and 2019 (a 36-year period).

4.1. Wetland dynamics in relation to other LULC changes between 1983 and 2019

The findings obtained from the study showed that the Maungani wetland has been subjected to continuous decline over the last 36 years (1983–2019). The wetland shrunk by 74.94% between 1983 and 2019. On the other hand, the built-up areas continuously expanded into the wetland area, and it was confirmed that 10.40% of wetland was lost to these areas. The loss of wetland to built-up areas is mainly attributed to population growth in the area, which increases demand for land for residential purposes or economic development in the vicinity of Maungani. In agreement with the 2011 census data, the national population, which includes the Maungani local community, was reported to have increased to 51.8 million in 2011 (STATSSA 2011). Other studies have also shown that the built-up areas are one of the major threats to unprotected wetland ecosystems. Wang et al. (2012), for example, revealed that urbanisation and the influx of migrants have

resulted in a sharp decline in regional ecological land in China. The ecological value of wetland ecosystems that occur in areas with a rapid population growth and economic development is lower, as in the Maungani area; however, a similar effect has been observed in other countries such as Ethiopia and Zimbabwe (Dubeau et al. 2017; Marambanyika et al. 2017). As depicted by the 1983 image, the population growth rate was low to the south and to the east of the wetland, when compared to high influx in the built-up areas in 2019, which shows the influence of the rapid population growth.

On the other hand, the least areal coverage of wetland was converted to forest, bare land and other vegetation, from 2000 to 2019, with 3.41%, 8.60% and 9.24%, respectively. During the study period, it was also observed that there was a gradual increase in the deterioration of the wetland near the built-up area south-east of it, when compared to other areas of the study. The increase in infrastructural development in the built-up area fuelled the loss of the spatial extent of the wetland. This is due to the flat terrain, because when the wetland gets dry, people occupy and develop the land. The drying of the land is associated with the decreased precipitation pattern and increased climatic conditions, as a result of climate change, which puts pressure on the extent of the wetland. Furthermore, human interference worsened the ecological condition of the Maungani wetland. Despite the high loss of its spatial extent, the wetland gained 2.37% from other vegetation and 0.92% from water. The wetland lost its major cover and other land cover types, such as water (37.08%), forest (33.99%), cultivated land (25.16%), as well as bare land (26.15%). In 2015, it was observed that there was an increase in the development of settlements to the south-east of the wetland, when compared to other portion of the study. Bare land dominated the north-east of the study area and, in 2019, a large portion of this area was converted to a built-up area. Urban development has a major influence on wetland shrinkage. Similar trends were observed in other parts of the continent. Studies by Sithole and Goredema (2013), Mhlanga et al. (2014) and Chikodzi and Mufori (2018) showed that human activities transformed the wetland hydrology in parts of the Harare metropolitan district in Zimbabwe, reducing their spatial extent, as these ecosystems were replaced by buildings or developments that affected the wetland retention, and eventually led to a loss of habitat for the aquatic species. In South Africa, Phethi and Gumbo (2019) found that poverty and population growth were the driving forces behind wetland mismanagement. They revealed that the cultivation of crops, road construction and built-up development, during the period from 1978 to 2004, were the main activities that contributed to the deterioration of the Makhitha wetland, located in the Limpopo Province. Climate change, built-up areas and agricultural activities were found to be the major factors that replace the extent of wetlands.

4.2. Long-time wetland monitoring using Landsat data

Mapping the spatial patterns of wetland areas over time is critical for detecting and monitoring the LULC changes and for understanding their effects on the integrity and ecological functioning of the wetland. The use of a freely accessible, accurate and reliable remote sensing dataset i.e., Landsat, with a 30-m spatial resolution, has enabled the mapping of the spatial extent of LULC in unprotected wetlands that are surrounded by rural communities. This will enable researchers and other wetland managers to investigate the spatial transformation of wetland over particular time periods (i.e., 1983–2019). Our approach supplements the wetland characterization systems that have demonstrated the use of multi-temporal mapping of wetland areas for understanding the pattern of LULC changes degrading wetland ecosystems (Gómez-Rodríguez et al. 2010; Knight et al. 2013;

Rover et al. 2011). Gabrielsen et al. (2016) employed a time-series approach in their analysis, which resulted in temporal wetland predictions regarding the probability of wetland inundation, and it successfully characterises wetlands as ephemeral inclines. Their strategy effectively used high- and moderate-resolution data to measure the likelihood of wetland inundation and the prospect that wetlands may be wet over time. Multi-temporal approaches derived by Gabrielsen et al. (2016) produced lower prediction errors of Rapid Eye 3.1–15% and Landsat 0.3–1.5% in the Northern Great Plains of the USA.

The Landsat data series has shown its capabilities for depicting and accurately mapping complex wetland areas and the surrounding LULC dynamics. The information depicted by Landsat images is critical for aquatic and wetland management and decision-making, especially in regions that have a restricted network system of field observation frameworks in place (Thamaga and Dube 2019). The findings of this study are consistent with previous investigations, and they underscore the precision and strength of using Landsat data for long-term mapping in wetland-related studies, LULC quantification, biomass estimation, crop and fire mapping, aquatic plant species and urban development (Dube et al. 2018; Dube and Mutanga 2015; Rampheri et al. 2022). Jin et al. (2017) demonstrated the unique strength and superiority of Landsat missions, as well as their practical viability in accurately mapping, detecting and monitoring the spatio-temporal changes for wetland assessment over-time. Although the imagery has been used in larger areas, particularly the wetlands recognised by the Ramsar Convention (Mozumder and Tripathi 2014), its application in small and unprotected wetlands serving the surrounding communities remains limited and under-studied. This demonstrated the ability of Landsat to map wetland conditions, using publicly available data, especially in data-scarce regions, such as in the semi-arid tropical regions of the sub-Saharan Africa. In addition, this would greatly assist in accurately deriving, monitoring, and reporting on the health condition and rate of degradation of wetlands.

Although the study provides an insightful overview of the state of unprotected wetlands in the arid-tropical regions of sub-Saharan Africa, the understanding of these ecosystems could be better depicted through the integration of multi-source data, including the perceptions of indigenous communities as well as seasonal dynamics. In addition, considering that wetland LULC characterisation was done by using broadband and spatial resolution satellite data, some inherent changes could have been missed. The 30-m spatial resolution of Landsat is associated with spectral mixing, which results in its poor discrimination ability. In this regard, spatially explicit methodologies that focus on analysing changes in the soil moisture, different types of vegetation or indices, as well high-resolution data must be explored. More so, there is a need to include climatic and soil data, so as to determine whether these changes are solely linked to anthropogenic activities. For example, the study showed that there was also an increase in vegetation (bush encroachment) in the wetland and that this may be due to climate variability and climate change (Bhaga et al. 2020). A review study by Bhaga et al. (2020) demonstrated that climate variability and recurrent droughts have caused remarkable strain on water resources in most regions across the globe, with the arid and semi-arid areas being the hardest hit and that this is likely to have an effect on the wetland conditions. This assertion is further strengthened by the work of Gxokwe et al. (2020), who noted that wetlands are degrading at a rapid rate globally, due to the environmental changes. Lastly, it was assumed that the provision of information on the accuracy of individual maps is likely to be insufficient, and hence there is a need for further studies to consider accuracy assessment of land use change, by using stratified estimation (Olofsson et al., 2023; Olofsson et al. 2014). Robust and transparent statistical approaches for assessing accuracy and estimating the areas of

change are critical for ensuring the integrity of land change information. It is therefore imperative to adopt the holistic monitoring of wetlands, as well as an assessment framework that includes climate and environmental data, etc., in the long-term mapping and modelling of wetland changes and their possible degradation.

4.3. Implications for wetland conservation and LULC management

The complexities of wetland ecohydrological processes necessitate a profound interpretation of LULC transition, as these changes influence the spatial extent of wetlands, their diversity, the waterflow, and ultimately, the proliferation of alien plant species. According to the findings of this study, the extent of the wetland ecosystem area is diminishing rapidly. This information provides the requisite baseline information required by environmental and wetland managers to devise sustainable intervention measures and strategies to curb the further deterioration of ecohydrological systems from the possible threats emanating from both anthropogenic and natural causes. These necessitate responsive management strategies to stop or reverse the rate of degradation or loss of wetlands, especially unprotected wetlands that have been overlooked in policy formulation. Increased management strategies, with an emphasis on wetland rehabilitation and restoration, are not backed up by adequate integrated data collection, reliable information and reviews. Uncertainty over the previous policy outcomes for LULC change and wetlands, as well as recent attempts to strengthen their protection, pose critical concerns about their ecological significance. Ecosystem managers need to strengthen their implementation policies to conserve wetland ecosystems, and to minimise the rate of their shrinkage, the extension of urban landscape patterns must be regulated.

4. Conclusions

This work explored the impacts of LULC change on wetland ecosystems in the Maungani wetland, which is located in the semi-arid tropical regions of South Africa. The integrated time-series Landsat data and Support Vector Machine algorithm were used to depict and model the historical LULC, and wetland change for a period of 36 years (1983–2019) to overcome the degradation and to contribute towards the sustainable management of these wetland ecosystems. There has been a widespread conversion of wetlands during the period of study. Based on our findings, the following conclusions were drawn.

- The Maungani wetland has undergone significant changes in terms of the LULC change dynamics over the years (1983 to 2019).
- Derived thematic maps show that the degraded wetland size has been largely replaced by built-up areas.
- The Maungani wetland has shrunk dramatically from 1 073 500 ha (43.10%) in 1983 to 345 100 ha (13.85%) in 2019.

Overall, the findings of this study demonstrated the usefulness of historical and archival Landsat data series in quantifying the impact of LULC change on semi-arid wetlands. The Landsat data-series offers the novel, accessible and up-to-date information that is required for the accurate monitoring and quantifying the human footprint on wetlands and this information is useful for improved management of small wetlands, which provide livelihoods to rural communities. It was noted that Maungani wetland has been experiencing a steady deterioration over the past 36 years. The derived remotely-sensed LULC

for Maungani provides the requisite baseline information for further wetland modelling and developing a spatial explicit remotely-sensed framework for wetland monitoring in semi-arid areas. There is however a need to test this approach in other regions with similar climatic conditions to test its transferability and determine its operability.

Acknowledgements

Authors would like to thank the United State Geological Survey (USGS) for provision satellite imagery and University of the Western Cape in South Africa for creating and enabling environment for research. We would also like to express our gratitude to the South African National Space and Agency (SANSA) for sponsoring this study. Finally, would like to thank Empire Partner Foundation (EPF) Tech Hub for supporting this study.

Disclosure statement

No conflict of interest.

ORCID

Kgabo Humphrey Thamaga http://orcid.org/0000-0002-2305-9975
Timothy Dube http://orcid.org/0000-0003-3456-8991
Cletah Shoko http://orcid.org/0000-0003-4222-3539

References

Adam EMI, Mutanga O. 2009. Spectral discrimination of papyrus vegetation (*Cyperus papyrus L.)* in swamp wetlands using field spectrometry. ISPRS J Photogramm Remote Sens. 64(6):612–620.

Adelabu S, Mutanga O, Adam E, Sebego R. 2014. Spectral discrimination of insect defoliation levels in mopane woodland using hyperspectral data. IEEE J Sel Top Appl Earth Observ Remote Sens. 7(1): 177–185.

Adeli S, Salehi B, Mahdianpari M, Quackenbush LJ, Brisco B, Tamiminia H, Shaw S. 2020. Wetland monitoring using SAR data: a meta-analysis and comprehensive review. Remote Sens. 12(14):2190.

Adjorlolo C, Mutanga O, Cho MA, Ismail R. 2013. Spectral resampling based on user-defined inter-band correlation filter: C3 and C4 grass species classification. Int J Appl Earth Obs Geoinf. 21:535–544.

Bassi N, Kumar MD, Sharma A, Pardha-Saradhi P. 2014. Status of wetlands in India: a review of extent, ecosystem benefits, threats and management strategies. J Hydrol: Reg Stud. 2:1–19.

Basu T, Das A, Pham QB, Al-Ansar N, Linh NTT, Lagerwall G. 2021. Development of integrated peri-urban wetland degradation assessment approach for the Chartra Wetland in eastern India. Sci Rep. 11(4470).

Bhaga TD, Dube T, Shekede MD, Shoko C. 2020. Impacts of climate variability and drought on surface water resources in Sub-Saharan Africa using remote sensing: a review. Remote Sens. 12(24):4184.

Calhoun AJK, Mushet DM, Bell KP, Boix D, Fitzsimons JA, Isselin-Nondedeu F. 2017. Temporary wetlands: challenges and solutions to conserving a disappearing ecosystem. Biol Conserv. 211:3–11.

Chandler HC, McLaughlin DL, Gorman TA, McGuire KJ, Feaga JB, Haas CA. 2017. Drying rates of ephemeral wetlands: implications for breeding amphibians. Wetlands. 37(3):545–557.

Chatziantoniou A, Psomiadis E, Petropoulos G. 2017. Co-orbital Sentinel 1 and 2 for LULC mapping with emphasis on wetlands in a Mediterranean setting based on machine learning. Remote Sens. 9(12): 1259.

Chen Y, Qiao S, Zhang G, Xu YJ, Chen L, Wu L. 2020. Investigating the potential use of Sentinel-1 data for monitoring wetland water level changes in China's Momoge National Nature Reserve. PeerJ. 8(8616).

Chikodzi D, Mufori RC. 2018. Wetland fragmentation and key drivers: a case of Murewa District of Zimbabwe. J Environ Sci Toxicol Food Technol. 12(9):49–61.

Connolly J. 2018. Mapping land use on Irish peatlands using medium resolution satellite imagery. Ir Geogr. 51(2):187–204.

Drusch M, Del Bello U, Carlier S, Colin O, Fernandez V, Gascon F, Hoersch B, Isola C, Laberinti P, Martimort P, et al. 2012. Sentinel-2: ESA's optical high-resolution mission for GMES operational services. Remote Sens Environ. 120:25–36.

Dubeau P, King JK, Unbushe DG, Rebelo LM. 2017. Mapping the Dabus wetlands, Ethiopia, using random forest classification of Landsat, PALSAR and Topographic data. Remote Sens. 9(10):1056.

Dube T, Mutanga O. 2015. Evaluating the utility of the medium-spatial resolution Landsat 8 multispectral sensor in quantifying aboveground biomass in uMgeni catchment, South Africa. ISPRS J Photogram Remote Sens. 101:36–46.

Dube T, Sibanda M, Bangamwabo V, Shoko C. 2018. Establishing the link between urban land cover change and the proliferation of aquatic hyacinth (*Eichhornia crassipes*) in Harare Metropolitan, Zimbabwe. Phys Chem Earth. 108:19–27. [CrossRef][10.1016/j.pce.2018.09.010]

Fashae OA, Olusola AO, Obateru RO, Adagbasa EG. 2020. Land use/land cover change and land surface temperature of Ibadan and environs. Environ Monit Assess. 192(2):109.

Gabrielsen CG, Murphy MA, Evans JS. 2016. Using a multiscale, probabilistic approach to identify spatial-temporal wetland gradients. Remote Sens Environ. 184:522–538.

Gallant AL. 2015. The challenges of remote monitoring of wetlands. Remote Sens. 7(8):10938–10950.

Gómez-Rodríguez C, Bustamante J, Díaz-Paniagua C. 2010. Evidence of hydroperiod shortening in a preserved system of temporary ponds. Remote Sensing. 2(6):1439–1462.

Goodin DG, Anibas KL, Bezymennyi M. 2015. Mapping land cover and land use from object-based classification: an example from a complex agricultural landscape. Int J Remote Sens. 36(18):4702–4723.

Gxokwe S, Dube T, Mazvimavi D. 2020. Multispectral remote sensing of wetlands in semi-arid and arid areas: a review on applications, challenges and possible future research directions. Remote Sens. 12(24): 4190.

Hagolle O, Sylvander S, Huc M, Claverie M, Clesse D, Dechoz C, Lonjou V, Poulain V. 2015. SPOT-4 (take 5): simulation of sentinel-2 time series on 45 large sites. Remote Sensing. 7(9):12242–12264.

Hettiarachchi M, Morrison TH, McAlpine C. 2015. Forty-three years of Ramsar and urban wetlands. Global Environ Change. 32:57–66.

Horwitz P, Finlayson CN. 2011. Wetlands as setting for human health: incorporating ecosystem services and health impact assessment into water resource management. BioScience. 61(9):678–688.

Immitzer M, Vuolo F, Atzberger C. 2016. First experience with sentinel-2 data for crop and tree species classifications in Central Europe. Remote Sens. 8(3):166.

IPBES. 2018. Summary for policymakers of the regional assessment report on biodiversity and ecosystem services for Europe and Central Asia of the intergovernmental science-policy platform on biodiversity and ecosystem services. In: Fischer M, Rounsevell M, Torre-Marin Rando A, Mader A, Church A, Elbakidze M, Elias V, Hahn T, Harrison PA, Hauck J, Martín-López B, Ring I, Sandström C, Sousa Pinto I, Visconti P, Zimmermann NE, Christie M, editors. IPBES secretariat. Bonn, Germany; p. 48..

Jia K, Wei X, Gu X, Yao Y, Xie X, Li B. 2014. Land cover classification using Landsat 8 operational land imager data in Beijing, China. Geocarto Int. 29(8):941–951.

Jin H, Huang C, Lang MW, Yeo I-Y, Stehman SV. 2017. Monitoring of wetland inundation dynamics in the Delmarva Peninsula using Landsat time-series imagery from 1985 to 2011. Remote Sens Environ. 190:26–41.

Kashaigili JJ, Majaliwa AM. 2013. Implications of land use and land cover changes on hydrological regimes of the Malagarasi River, Tanzania. JASA. 02 (01):45–50.

Knight JF, Tolcser BP, Corcoran JM, Rampi LP. 2013. The effects of data selection and thematic detail on the accuracy of high spatial resolution wetland classifications. Photogramm Eng Remote Sens. 79(7): 613–623.

Lambin EF, Meyfroidt P. 2010. Land use transitions: socio-ecological feedback versus socio-economic change. Land Use Policy. 27(2):108–118.

Lee JC, Menalled FB, Landis DA. 2001. Refuge habitats modify impact of insecticide disturbance on carabid beetle communities. J Appl Ecol. 38(2):472–483.

Licciardi G, Pacifici F, Tuia D, Prasad S, West T, Giacco F, Thiel C, Inglada J, Christophe E, Chanussot J, et al. 2009. Decision fusion for the classification of hyperspectral data: outcome of the 2008 GRS-S data fusion contest. IEEE Trans Geosci Remote Sens. 47(11):3857–3865.

Ligate EJ, Chen C, Wu C. 2018. Evaluation of tropical coastal land cover and land use changes and their impacts on ecosystem service values. Ecosyst Health Sustain. 4(8):188–204.

Lin Y, Yu J, Cai J, Sneeuw N, Li F. 2018. Spatio-temporal analysis of wetland changes using a kernel extreme learning machine approach. Remote Sens. 10(7):1129.

Malak DA, Hilarides L. 2016. Guidelines for the delimitation of wetland ecosystems. ETC-UMA: Málaga, Spain:1–23.

Mansaray LR, Yang L, Kabba VTS, Kanu AS, Huang J, Wang F. 2019. Optimising rice mapping in cloud-prone environments by combining quad-source optical with Sentinel-1A microwave satellite imagery. GIScience Remote Sens. 56(8):1333–1354.
Marambanyika T, Beckedahl H, Ngetar NS, Dube T. 2017. Assessing the environmental sustainability of cultivation systems in wetlands using the WET-health framework in Zimbabwe. Phys Geogr. 38(1): 62–82.
Materu SF, Urban B, Heise S. 2018. A critical review of policies and legislation protecting Tanzanian wetlands. Ecosyst Health Sustain. 4(12):310–320.
Mhlanga B, Maruziva R, Buka L. 2014. Mapping wetland characteristics for sustainable development in Harare: The case of Borrowdale west, Highlands, National sports stadium and Mukuvisi woodlands wetlands. Ethiop J Env Stud Manag. 7(5):488–498.
Mohammadimanesh F, Salehi B, Mahdianpari M, Brisco B, Motagh M. 2018. Multi-temporal, multi-frequency, and multi-polarization coherence and SAR backscatter analysis of wetlands. ISPRS J Photogramm Remote Sens. 142:78–93.
Mozumder C, Tripathi NK. 2014. Geospatial scenario-based modelling of urban and agricultural intrusions in Ramsar wetland Deepor Beel in Northeast India using a multi-layer perceptron neural network. Int J Appl Earth Obs Geoinf. 32:92–104.
Muavhi N. 2020. Evaluation of the effectiveness of supervised classification algorithms in land cover classification using ASTER images – A case study from the Mankweng (Turfloop) area and its environs, Limpopo Province, South Africa. South Afr J Geomat. 9(1).
Muavhi N. Mavhungu 2020. Mapping of gold-related alteration minerals and linear structures using ASTER data in the Giyani Greenstone Belt, South Africa. South Afr J Geomat. 9(2).
Mudereri BT, Dube T, Adel-Rahman EM, Niassy S, Kimathi E, Khan Z, Landmann T. 2019. A comparative analysis of PlanetScope and Sentinel-2 space-borne sensors in mapping Striga weed using Guided regularised random forest classification ensemble. The International Archives of the Photogrammetry, Remote Sensing and Spatial Information Sciences, Volume XLII-2/W13, 2019. ISPRS Geospatial Week2019, 10–14 June, Enschede, The Netherlands.
Munishi S, Jewitt G. 2019. Degradation of kilombero valley Ramsar wetlands in Tanzania. Phys Chem Earth, Parts A/B/C. 112:216–227.
Munyati C. 2000. Wetland change detection on the Kafue Flats, Zambia, by classification of a multitemporal remote sensing image data. Int J Remote Sens. 21(9):1787–1806.
Mushore TD, Mutanga O, Odindi J, Dube T. 2016. Assessing the potential of integrated Landsat 8 thermal bands, with the traditional reflective bands and derived vegetation indices in classifying urban landscapes. Geocarto Int.:1–34.
Nkonya E, Mirzabaev A, von Braun J. (eds). 2016. Economics of land degradation and improvement: a global assessment for sustainable development. Cham: Springer.
Olofsson P, Foody GM, Herold M, Stehman SV, Woodcock CE, Wulder MA. 2014. Good practices for estimating area and assessing accuracy of land change. Remote Sens Environ. 148:42–57.
Pontius RG, Jr., Millones M. 2011. Death to kappa and to some of my previous work: a better alternative. Int J Remote Sens. 32(15):4407–4429.
Rampheri M, Dube T, Dhau I. 2022. Use of remotely sensed data to estimate tree species diversity as an indicator of biodiversity in Blouberg Nature Reserve, South Africa. Geocarto Int. 37(2):526–542.
Rebelo LM, McCartney MP, Finlayson CM. 2010. Wetlands of Sub-Saharan Africa: distribution and contribution of agriculture of livelihoods. Wetlands Ecol Manage. 18(5):557–572.
Robertson L, King D, Davies C. 2015. Object-based image analysis of optical and radar variables for wetland evaluation. Int J Remote Sens. 36(23):5811–5841.
Rover J, Wright C, Euliss N, Mushet D, Wylie B. 2011. Classifying the hydrologic function of prairie potholes with remote sensing and GIS. Wetlands. 31 (2):319–327.
Sahu SK, Prasad MBNV, Tripathy BK. 2015. A support vector machine binary classification and image segmentation of remote sensing data of Chilika Lagloon. Int J Res Inf Technol. 3(5):191–204.
Schuyt KD. 2005. Economic consequences of wetland degradation for local populations in Africa. Ecol Econ. 53(2):177–190.
Siachalou S, Doxani G, Tsakiri-Strati M. 2014. Time-series analysis of high temporal remote sensing data to model wetland dynamics: a hidden Markov Model approach. In Proceedings of the SENTINEL-2 for Science Workshop—ESA-ESRIN, Frascati, Italy, p. 20–22. May 2014.
Singh SK, Srivastava PK, Szabo S, Petropoulos GP, Gupta M, Islam T. 2016. Landscape transform and spatial metrics for mapping spatiotemporal land cover dynamics using Earth observation datasets. Geocarto Int.:1–15.

Sithole A, Goredema B. 2013. Building in wetlands to meet the housing demands and urban growth in Harare. Int J Human Soc Sci. 3(8).

Slagter B, Tsendbazar NE, Vollrath A, Reiche J. 2020. Mapping wetland characteristics using temporally dense Sentinel-1 and Sentinel-2 data: a case study in St. Lucia wetlands, South Africa. Int J Appl Earth Observ Geoinf. 86(102009).

STATSSA 2011. Statistics South Africa, http://www.statssa.gov.za/?page_id=964.

Symeonakis E, Drake N. 2004. Monitoring desertification and land degradation over sub-Saharan Africa. Int J Remote Sens. 25(3):573–592.

Thamaga KH, Dube T. 2019. Understanding the seasonal mapping of invasive water hyacinth (Eichhornia crassipes) in the Greater Letaba river system using Sentinel-2 satellite data. GIScience Remote Sens. 56(8):1355–1377.

Thamaga KH, Dube T, Shoko C. 2021. Advances in satellite remote sensing of the wetland ecosystems in Sub-Saharan Africa. Geocarto Int.:1–21.

Tiner, R.W., Lang, M.W. & Klemas, V.V. (Eds.), 2015. Remote sensing of wetlands: applications and advances. CRC Press.

Van Asselen S, Verburg PH, Vermaat JE, Janse JH. 2013. Drivers of wetland conversion: a global meta-analysis. PLoS One. 8 (11):e81292.

Wang L, Dronova I, Gong P, Yang WB, Li YR, Liu Q. 2012. A new time series vegetation–water index of phenological–hydrological trait across species and functional types for Poyang Lake wetland ecosystem. Remote Sens Environ. 125:49–63.

Yirsaw E, Wu W, Shi X, Temesgen H, Bekele B. 2017. Land use land cover change modelling and the prediction of subsequent changes in ecosystem service values in the coastal area of China, the Su-Xi-Chang region. Sustainability. 9(7):1204–1217.

Yu X, Zhang A, Hou X, Li M. 2013. Multi-temporal remote sensing of land cover change and urban sprawl in the coastal city of Yantai, China. Int J Digital Earth. :37–41.